

DETECTION AND SEGMENTATION OF LUNGS REGIONS USING CNN COMBINED WITH LEVELSET

Pedro Cavalcante Sousa Júnior , **Luís Fabrício de Freitas Souza** ,

José Jerovane da Costa Nascimento 

Instituto Federal de Educação, Ciência e Tecnologia do Ceará - IFCE, CE

Universidade Federal do Ceará - UFC, CE

LAPISCO-Laboratório De Processamento de Imagem, Sinais e Computação Aplicada, (e-mail: coord@lapisco.ifce.edu.br)

{pedro.cavalcante, fabricio.freitas, jerovane.nascimento}@lapisco.ifce.edu.br

Lucas Oliveira dos Santos , **Adriell Gomes Marques** ,

Francisco Eduardo Sales Ribeiro ,

Pedro P. Rebouças Filho 

Instituto Federal de Educação, Ciência e Tecnologia do Ceará - IFCE, CE

LAPISCO-Laboratório De Processamento de Imagem, Sinais e Computação Aplicada, (e-mail: coord@lapisco.ifce.edu.br)

{lucas.santos, adriell.gomes}@lapisco.ifce.edu.br,

francisco.eduardo.sales62@aluno.ifce.edu.br, pedrosarf@ifce.edu.br

Abstract – Lung diseases are among the leaders in ranking diseases that kill the most globally. A quick and accurate diagnosis made by a specialist doctor facilitates the treatment of the disease and can save lives. In recent decades, an area that has gained strength in computing has been the aid to medical diagnosis. Several techniques were created to help health professionals in their work using Computer Vision Techniques and Machine Learning. This work presents a method of lung segmentation based on deep learning and computer vision techniques to aid in the medical diagnosis of lung diseases. The method uses the Detectron2 convolutional neural network for detection, which obtained 99.89% accuracy for detecting the pulmonary region. It was then combined with the LevelSet method for segmentation, which got 99.32% accuracy in segmentation in Lung Computed Tomography images being equivalent in state of the art, surpassing different deep learning models for segmentation.

Keywords – Medical Images, Computed Tomography, Deep Learning, Pulmonary Detection and Segmentation.

1. INTRODUCTION

According to the World Health Organization (WHO) [1], lung diseases are some of the leading causes of mortality around the world, being classified as a public health problem. Among the pulmonary diseases, chronic obstructive pulmonary diseases (COPD), tuberculosis, and lung cancer stand out. More than 200 million individuals have been estimated to suffer from COPD around the world [2]. In addition, tuberculosis and lung cancer also have alarming numbers. According to WHO [3] in 2020, there were more than 10 million new cases of tuberculosis around the world, and it was responsible for more than 1.5 million deaths in 2020.

Lung cancer is the type of cancer that kills the most in the world [4], according to the WHO, lung cancer is the second leading cause of death before age 70. According to Sung *et al.*, in 2020, there were more than 2 million new lung cancer cases worldwide. The authors also found that the number of deaths caused by lung cancer was close to 1.8 million. In addition, lung cancer ranks second in the ranking of most diagnosed cancer [4]. Therefore, lung cancer is one of the primary diseases that specialist doctors have to deal with daily.

Lung diseases directly impact people's quality of life and life expectancy. Effective treatment requires the condition to be diagnosed in its early stages [5]. A specialist doctor is responsible for making the diagnosis. The professional analyzes computed tomography (CT) images to make the diagnosis and initiate treatment [6]. The first step towards an accurate diagnosis of lung disease is the segmentation of the lung region of interest (ROI) on computed tomography (CT) [6]. However, most of the time, segmentation is manual work performed by the doctor, bringing fatigue and loss of precious time to their work. However, computing techniques can automate the segmentation process to make your job easier.

Therefore, one of the main focuses of the researchers is to help medical diagnosis, seeking speed and accuracy in the diagnosis through the use of artificial intelligence for CT segmentation. In recent years researchers have developed several techniques using digital image processing and artificial intelligence (AI) [7] [8] [9] to perform this segmentation automatically and facilitate the professional's work. Such methods have satisfactory effectiveness and good confidentiality; however, these methods can be improved.

Furthermore, machine learning techniques need reliable and accurate data to have good training and obtain satisfactory results [10]. Therefore, creating detailed, highly segmented images becomes a crucial point for training Machine Learning

models and applying these techniques. Given the problem, this work proposes an automatic and efficient lung segmentation method based on a neural network called Detectron2 combined with digital image processing and LevelSet techniques.

1.1 Related Works

In this section, we will present works that cover our research area, from pure DIP techniques to the application of complex machine learning algorithms.

Digital image processing (DIP) techniques consist of manipulating the values of an image through mathematical operations. Computer vision techniques have several applications, such as facial recognition, object detection systems, and image pre-processing, among others [11]. One of the applications in which computer vision stands out is as an aid to medical diagnosis [12].

Li *et al.* [13] proposed a segmentation method based on DIP techniques using LevelSet together with fuzzy logic. First, the authors use fuzzy clustering to supervise the LevelSet initialization. After that, they apply balloon force and growth of regions. Therefore, the ROI increment occurs, and the segmentation is performed. The authors used their method for different types of images. Regarding the segmentation of medical images, the authors reach 84.2% of accuracy. However, the authors did not compare their results to expert targeting, so their metrics do not have high reliability.

Rebouças F F. *et al.* [14] developed a method based on the active contour technique for lung segmentation and brain stroke segmentation. The authors used the active boundary theory in combination with an internal and external energy technique based on the Optimum Path Forest Classifier that performs a neighborhood analysis at each point and suggests the right path to follow—the method named by the author's Optimum Path Snakes(OPS). The authors obtained metrics above 80% of Dice's coefficient for segmentation of stroke and metrics of 91% of Dice's coefficient for segmentation of the pulmonary region in CT.

Gupta *et al.* [15] proposed a method to classify a CT image as sick or healthy. The method proposed by the authors consists of combining evolutionary algorithms such as the Improvised Crow Search Algorithm (ICSA), Improvised Gray Wolf Algorithm (IGWA), and the Improvised Cuttlefish Algorithm (ICFA) with machine learning techniques for CT classification. The authors' approach uses evolutionary algorithms as a feature selection for machine learning algorithms, thus reducing the computational cost of machine learning algorithms. As a result, they found that the ICSA eliminated most of the irrelevant features 71%. However, the best combination for the pulmonary classification was IGWA + KNN, which obtained 99.4% accuracy. However, the dataset used by the authors was tiny, containing only 36 TCS, which may have led to less reliable results.

Hu *et al.* [6] presented a study in which they applied deep learning techniques for lung segmentation. Using the Convolutional Neural Network (CNN) Mask R-CNN combined with classical machine learning classifiers to perform lung segmentation. The authors achieved 97.62% accuracy with the combination of Mask R-CNN with the unsupervised classifier Kmeans. However, the dataset used had only 39 images.

Skourt *et al.* [16] presented a method for lung segmentation using deep learning. The authors used the U-net architecture for image segmentation; U-net extracts attributes from the input images for its training and uses them to segment new input images in the test phase. The authors used the LIDC-IDRI [17] dataset. His method reached the metric of 95.02% of the Dice coefficient. However, the authors used only the Dice coefficient as a metric, so their results have little reliability.

Also motivated by the problem of segmentation of medical images, Han *et al.* [18] proposed a technique based on the health of things. The method can address different problems of segmentation. Since the input image is classified as to its type and then segmented, the technique can detect the input CT as being from the lung or brain affected by Hemorrhagic Stroke. Then, according to the pointed class, the method segments the AVC, or the lung, from the rest of the image with the help of the Detectron2 Network. The authors used two datasets for the construction of the model. The first consisted of 1265 CT scans of the chest and 100 images of Hemorrhagic CVA. In its results, the method obtained satisfactory results, with 97% of Dice and relatively fast segmentation time. However, it is worth mentioning the imbalance of the data set used and the lack of in-depth study about the effect of the number of iterations used in the network in question.

2. Materials and Methods

This section presents the materials and methods covered in this study and the evaluation metrics used to compare results.

2.1 Dataset

The dataset used in this study is composed of 1172 images in Portable Network Graphics (PNG) format of pulmonary CTS at 512×512. Each image has a Ground truth (GT) corresponding to the segmentation performed by a specialist doctor. The dataset was built and made available by the Walter Cândido Hospital of the Federal University of Ceará (UFC). The dataset was approved by the Research Ethics Committee, Committee - COMEPE (Protocol No. 35/06), this dataset was also used in previous articles [19] [20] [21] [22] [14] [18] [6].

2.2 Detectron2

This subsection describes the Detectron2 [23] tool used for detection of the lung region.

Detectron2 is a deep neural network derived from the MASK-RCNN [24] network, and the successor to Detectron [25] developed by Facebook AI Research [23]. Detectron2 can perform the detection, classification, and segmentation of objects of interest from its two-step operation. To train Detectron2 to address the selected problem, a relative amount of original images

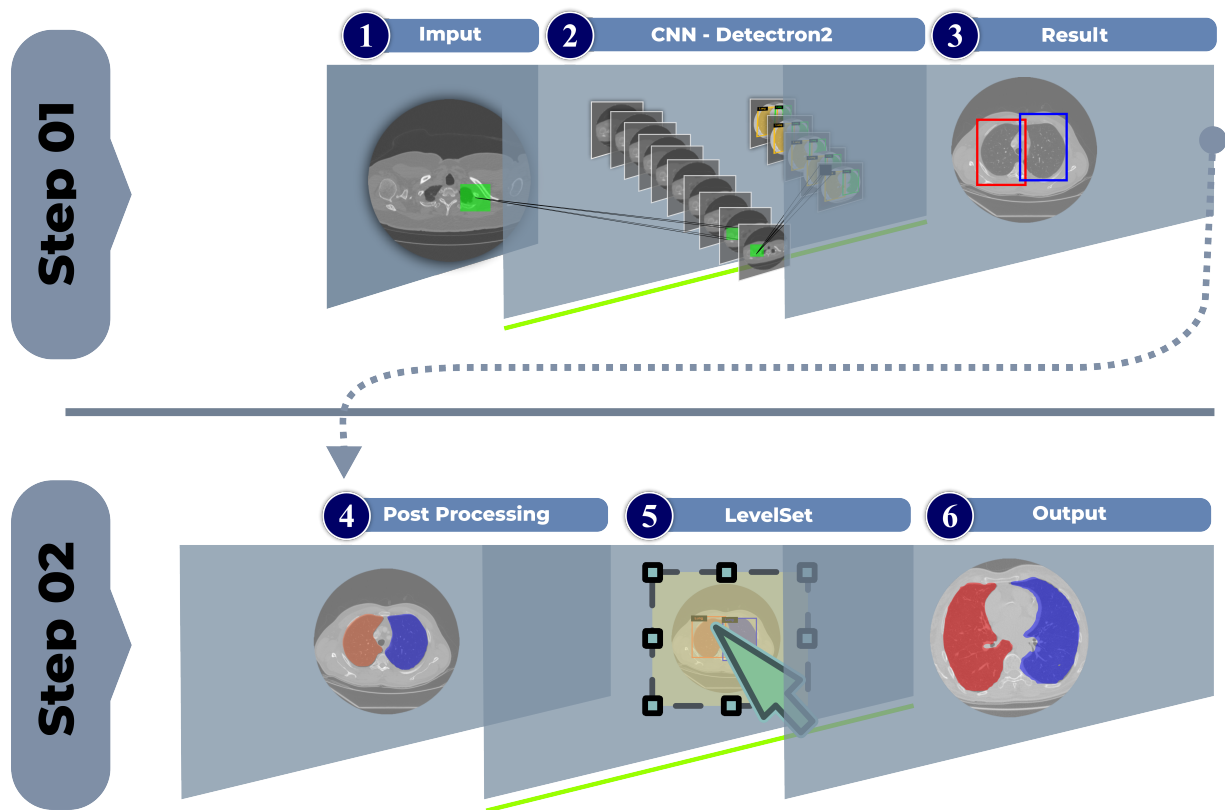


Figura 1: It presents the methodology of this study, which is divided into two stages; Detection Step (Image 1-Input: Input of the CT image into the model, Image 2-CNN Detectron2: Image detection process, and Image 3-Results: Results of detection through the bounding box), The Segmentation Step (Image 4-Post-Processing: Using Dilation of the output image in the previous step, Image 5-LevelSet Method: Process of readjusting the lung regions and Image 6-Final Result: Showing the segmentation of the Lungs.

and their respective GTs is necessary. Thus, with the help of the GTs in the training stage, the network can learn the attributes of the region of interest to the detriment of other parts of the image. The output of Detectron2 comprises the marking of the region of interest through bounding boxes, the binary mask of the segmented region, and the region class, with the respective method's certainty index in the labeling. [18]

After proper training of Detectron2, in the test stage, a set of images of the Dataset not used in training is sent, typically comprising 20% of the Dataset. Detectron2 performs the detection, classification, and segmentation of the region of interest in the image. Detectron2 chooses probable regions of interest (ROI) in the detection step by demarcating them by bounding boxes. One of the criteria for selecting these regions is the number of pixels with attributes similar to the regions of interest learned by the method during your workout. In the segmentation phase, the network analyzes the probable regions of interest listed in the detection phase, pixel by pixel. Classifying whether the pixel is part of the region of interest. After that, the network performs a binarization of the segmented region. The output becomes the binarized mask of that region [24]

2.3 LevelSet

This subsection describes the LevelSet method used for segmenting the lung region.

LevelSet is an effective method for locating edges, and the method is to use a plane of interest to make edge adjustments. The mask is set to the image of interest and used as a background for the method. The LevelSet creates a secondary plane on which it will act and adjust its edges using the mask of interest. The adjustments are made through symmetrical mathematical calculations. The secondary plane coordinates are then adjusted one by one, resulting in the delimitation of the region of interest [26].

2.4 Parzen Window

Parzen Window is a non-parametric method of estimating probability distributions from data labeled [27]. The technique uses mathematical calculations to estimate the probability of a given pixel being or not belonging to the ROI. The calculation uses a positive and fixed Kernel function to determine different weights for the elements corresponding to their distance from the field. The further an element is from the field, the smaller its weight [28].

The equation 1 mathematically describes Parzen Window. In the equation, we have $p(z)$ as the representation of the probability of a pixel belonging or not to the ROI in question, z is the pixel that is having its probability calculated, δ is the kernel function, h is the edge length, n is the total number of pixels in the region [28].

$$p(z) = \frac{1}{n} \sum_{i=1}^{nH} \delta_n(z - z_i) \quad (1)$$

2.5 Evaluation Metrics

Evaluation metrics are used to evaluate the efficiency and performance of [29] segmentation. The metrics we chose for this work are Accuracy(Acc), Sensitivity(Sen), Dice Coefficient (Dice), Specificity(Spe), Negative predictive value(Npv), and Positive predictive value (Ppv) .

Accuracy (Acc): The accuracy refers to the ratio of the total number of pixels correctly segmented by the total number of segmented pixels in the image [30] . In our case, it refers to the number of pixels of the segmentation result corresponding to the GT segmented by the doctor. The equation 2 demonstrates the accuracy. Where TN corresponds to true negatives, TP to true positives, FP false positives and FN false negatives.

$$Accuracy = \frac{TP + TN}{TP + TN + FP + FN} \quad (2)$$

Negative predictive value(Npv): Npv refers to the number of pixels correctly classified as the background of the image [31]. The equation 3 mathematically demonstrates the Npv.

$$Npv = \frac{TN}{TN + FN} \quad (3)$$

Positive predictive value (Ppv): Metric referring to the number of pixels correctly classified as part of the object of interest in the image [31]. The equation 4 demonstrates the Ppv metric mathematically.

$$Ppv = \frac{TP}{TP + FP} \quad (4)$$

Sensitivity (Sen): Metric refers to the number of positive values correctly classified as positive. In our case, it refers to the proportion of correctly segmented pixels as positive. The equation 5 refers to the formula for calculating the sensitivity [18].

$$Sensitivity = \frac{TP}{TP + FN} \quad (5)$$

Specificity (Spe): Metric referring to the number of negative values correctly classified as negative [32]. In our case, it refers to the number of pixels that did not correspond to the region and were correctly classified. The equation6 expresses specificity mathematically.

$$Specificity = \frac{TN}{TN + FP} \quad (6)$$

Dice Coefficient (Dice): Statistical metric calculates the similarity index between two data sets. In our case, it refers to the similarity between the segmentation result compared to its respect GT [33]. The Dice coefficient is mathematically expressed by 7.

$$Dice = \frac{2TP}{2TP + FP + FN} \quad (7)$$

3. Methodoly

This section describes the methodology of this work, which is divided into three stages; Training step, detection step, and segmentation step.

3.1 Training Stage

In this step, 1, the model training process is carried out using a CNN network, the convolutional network used in this study was the Detectron2 network, presented in the 2.2 section. According to the image representing the training of the model, the dataset shown in the 2.1 section is used, where the network receives as input the CT images belonging to the lung and their respective GT duly marked by specialist physicians, totaling 1172 images. Training is performed with 80% of the images, reserving 20% for testing. 10000 iterations were used to train the model, thus generating the pulmonary detection model.

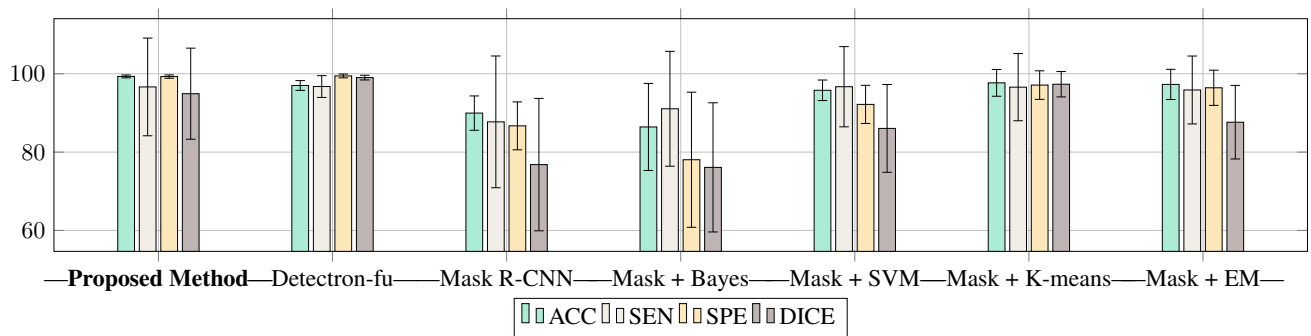


Figura 2: Graph of results compared with different models based on deep learning found in the literature.

3.2 Detection State

From the model generated for lung detection shown in Figure 1, detection of the lung region begins. In Figure 1, image 1, the process of detecting the object of interest (Lung Region) begins with the input of the CT image in the already trained model. In Figure 1, image 2, the trained model processes the input image, classifying each pixel as belonging or not to the region of interest, detecting the lung region through a bounding box. Detectron2 processes the input image during the testing stage to choose the possible bounding boxes based on the pixel similarities seen during training. Image 3 of Figure 1 presents the result of the input image detection process, ending the detection process. Detectron2 outputs two images for each input image, one of which is the chosen bounding box, and the other is its binarized mask.

After the detection result, the image goes on to the segmentation process, the third step of the proposed method.

3.3 Segmentation Stage: LevelSet

In this step, the segmentation step of our method is described. We use LevelSet techniques to perform the segmentation of the lung region.

Our approach is to use Detectron2's output as the growth mask for the LevelSet. First, as shown in Figure 1, image 4, we load the detection images from Detectron2 and apply a dilation with two iterations and kernel 3×3 . We use the dilation technique so that the LevelSet can make adjustments and perform segmentation of the lung region, as shown in Figure 1 image 5. Then we apply the parzen windowing technique on the dilated image, where the mask is adjusted, and the edges are refined. In Figure 1 image 6, the adjustment result is then used as the segmentation result.

4. Results

In this section, the results obtained during the stages of this study are presented.

4.1 Lung Detection

In this subsection, the detection results on the pulmonary region are presented. The 1 table presents different metric results for lung detection in CT.

The Detectron2 convolutional network showed excellent results for detecting lung regions, obtaining 99.30% accuracy, with a standard deviation of 0.47, demonstrating the excellent effectiveness for the detection problem in lung images on CTs. The accuracy indicated a general performance of the model with great efficiency, correctly classifying the region of interest, that is, where there are regions belonging to the lung and regions not belonging to the lung in the tomographic image. The same applied to the metrics (Npv) and (Spe); both metrics present excellent results above 99%, that is, the model can effectively detect regions that do not belong to the lung, making the model more accurate in detection through the bounding boxes, since the non-detection of regions delimits the delineation in the shape of the box through the adjustment to the region containing the lung. Thus, the model can identify the threshold between the end of the region where regions belonging to the lung and non-lung locations are located.

The Sensitivity (Sen) (Ppv) and (Dice) metrics obtained encouraging results for the detection problem. The detection of the region of interest (lung detection) achieved excellent results, obtaining 95% in (Sen), 97% in (Ppv), and (96%) in Dice, thus proving the effectiveness in detecting the lungs in images of pulmonary CT.

4.2 Lung segmentation

In this subsection, the results of lung segmentation are presented. The 2 table presents the metric values of performing the segmentation of the lung region.

The model accurately segmented different lung contours, obtaining excellent metric values with 99.32% accuracy and low standard deviation values. The metric values in the segmentation got values similar to the detection step; this was because the

Tabela 1: Pulmonary Detection Results.

Metrics	Detectron2
Acc	99.30 ± 0.47
Npv	99.46 ± 0.39
Sen	95.14 ± 8.93
Spe	99.68 ± 0.35
Ppv	97.46 ± 7.90
Dice	96.17 ± 8.10

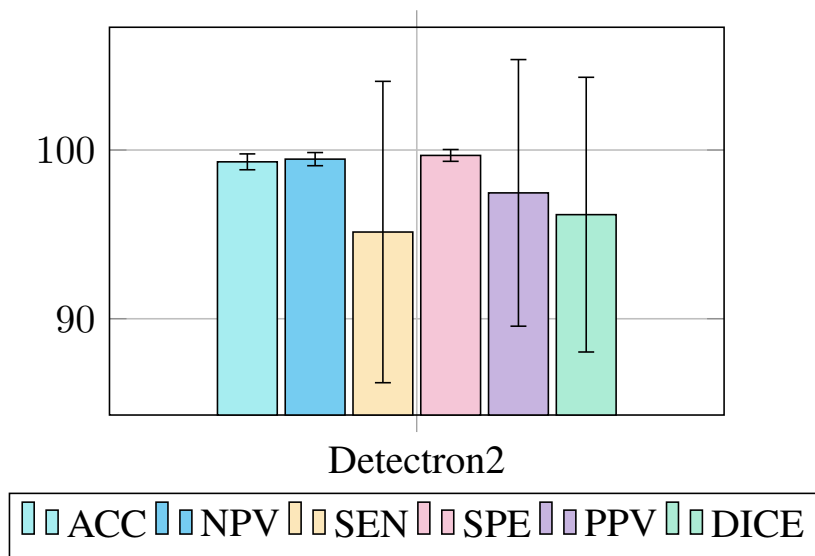


Figura 3: Pulmonary detection results graph.

segmentation process is carried out from the dilatation step in the detection output image. Thus, starting as a starting point for finding the different contours of the lung wall located on the CT image.

The metrics of (Sen), (Ppv), and (Dice) maintained a slight difference given by the degree of precision of the contours and the different problems in lung images. This fact is due to the involuntary process of breathing and inhaling from the lungs in the CT capture, which provides different images and challenging contours, as shown in Figure 5 with varying slices of lung regions captured by the CT scanner. The values obtained demonstrate this with 96.74% in the Sensitivity metric (Sen) and obtaining 93.42% for the (Ppv) metric for lung segmentation. From this testing stage, we seek to deepen the results with works found in the state of the art.

Tabela 2: Lung segmentation results.

Metrics	Detectron2
Acc	99.32 ± 0.37
Npv	99.89 ± 0.17
Sen	96.64 ± 12.47
Spe	99.28 ± 0.42
Ppv	93.42 ± 11.14
Dice	94.91 ± 11.63

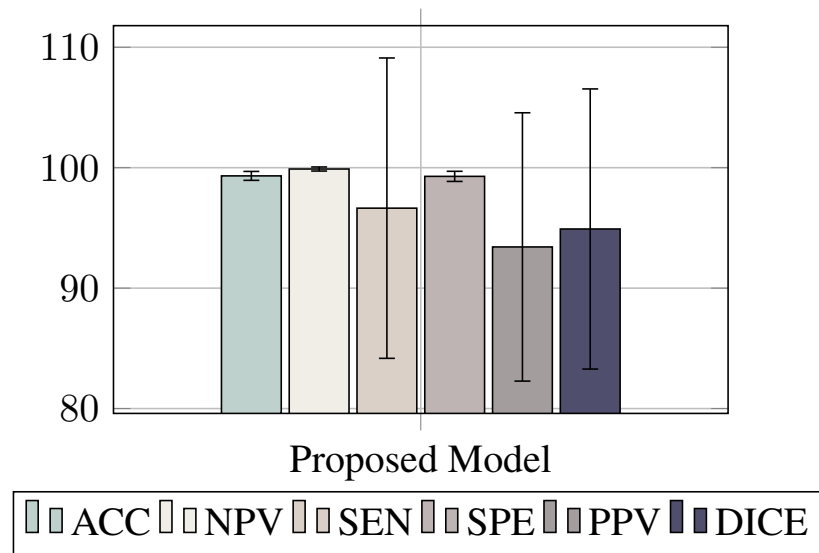


Figura 4: Graph of results compared with different models based on deep learning found in the literature.

4.3 Validation of results

This subsection presents the validation of the results obtained by comparing the results with different models based on deep learning found in the literature.

Table 3 presents different models based on deep learning for the problem of lung detection and segmentation in CT images. Both works used the same database. As can be seen, the proposed model obtained 99.32% of Accuracy (Acc), surpassing the works found in the literature, where it got a difference of more than 2% for the segmentation of the object of interest, including the slightest standard deviation reaching a 0.37 against 1.25 of the model in comparison (Model Detectron-fu). The metrics of (Sen) and (Spe) were similar compared to the Detectron-fu model of [18], obtaining a greater variation compared to the metric of (Dice).

Tabela 3: Results compared with state of the art.

	Acc	Sen	Spe	Dice
Metodo Proposto	99.32 ± 0.37	96.64 ± 12.47	99.28 ± 0.42	94.91 ± 11.63
Detectron-fu han2020internet	97.01 ± 1.25	96.74 ± 2.78	99.45 ± 0.49	99.02 ± 0.60
Mask R-CNN hu2020effective	89.96 ± 4.38	87.72 ± 16.82	86.70 ± 6.12	76.81 ± 16.90
Mask + Bayes hu2020effective	86.42 ± 11.11	91.06 ± 14.66	78.05 ± 17.25	76.10 ± 16.49
Mask + SVM hu2020effective	95.78 ± 2.62	96.69 ± 10.24	92.18 ± 4.87	86.05 ± 11.21
Mask + K-means hu2020effective	97.68 ± 3.42	96.58 ± 8.58	97.11 ± 3.65	97.33 ± 3.24
Mask + EM hu2020effective	97.28 ± 3.85	95.86 ± 8.67	96.42 ± 4.49	87.63 ± 9.39

Figure 5 shows detection using a bounding box in different slices of the lung tomography image, followed by segmentation by the proposed method, bypassing the lung walls. The model can identify and segment the two objects of interest at once. Therefore, making the model more robust.

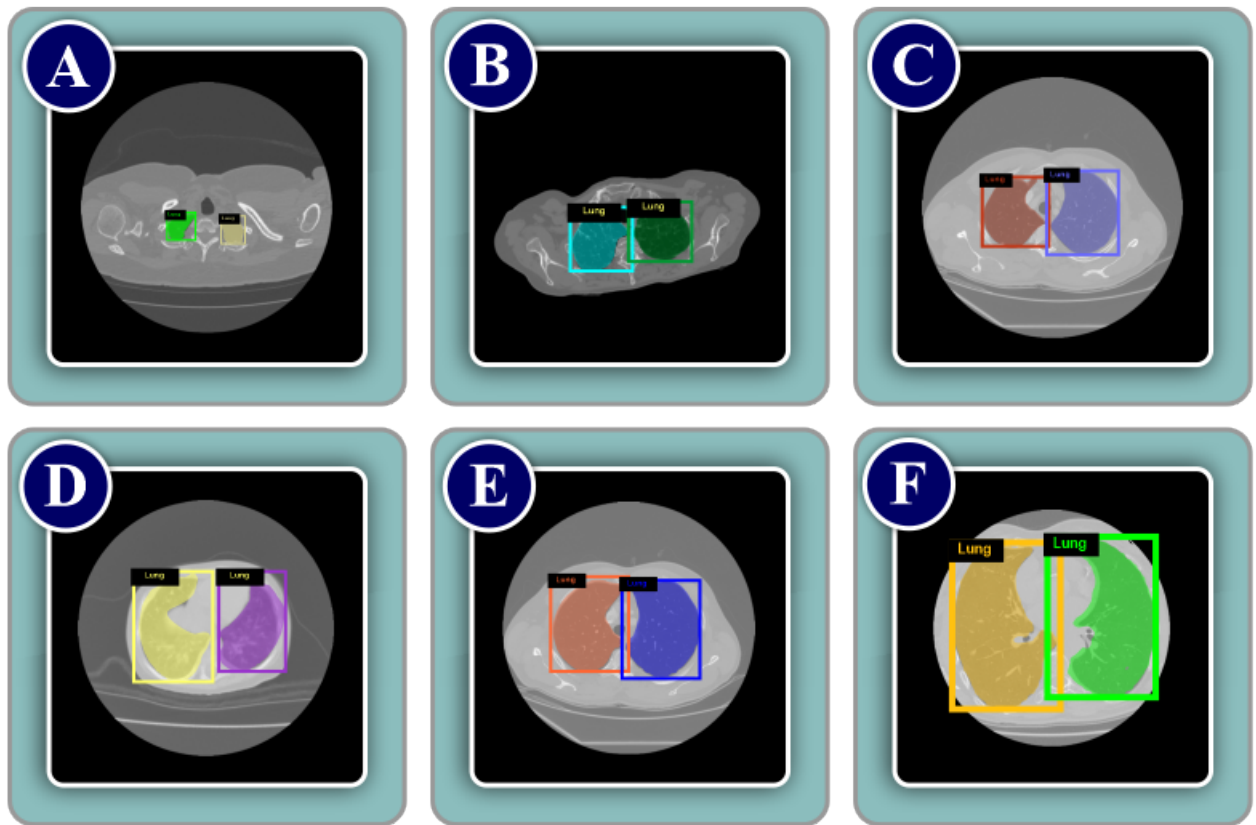


Figura 5: Results of segmentation of the proposed method for different chest CT slices

5 Conclusion

This study aimed to create an automatic and effective method for lung segmentation. In the first stage, we performed the DeepLearning model's training to detect the lung area. Then we use the detected mask to apply DIP and LevelSet techniques. For the application of the LevelSet, we used the dilation technique as image preprocessing.

We obtained satisfactory results, the pulmonary region in the tested images obtained the accuracy metric reached 99.32%, and the other metrics also achieved good results keeping all their values above 94%. Therefore, our approach made a precise segmentation from a detection mask.

This method opens space for better segmentation of lung images and aids in medical diagnosis. The specialist doctor can segment his regions of interest with high precision, thus saving manual and tiring work and using his time for situations of greater urgency and patient treatment.

However, our method can still be improved in some aspects of future research. It is necessary to use it in other databases with different DIP techniques for robust analysis of the results. In addition, the proposed method must also be tested to perform the segmentation of different types of medical images as other organs to validate the generalization of the technique.

Acknowledgments

This study was financed in part by the Coordenação de Aperfeiçoamento de Pessoal de Nível Superior - Brasil (CAPES) - Finance Code 001". Also Pedro Pedrosa Rebouças Filho acknowledges the sponsorship from the Brazilian National Council for Research and Development (CNPq) via Grants Nos. 431709/2018-1 and 311973/2018-3.

REFERENCES

- [1] W. H. Organization. *Global tuberculosis report 2013*. World Health Organization, 2013.
- [2] R. Lozano, M. Naghavi, K. Foreman, S. Lim, K. Shibuya, V. Aboyans, J. Abraham, T. Adair, R. Aggarwal, S. Y. Ahn *et al.*. “Global and regional mortality from 235 causes of death for 20 age groups in 1990 and 2010: a systematic analysis for the Global Burden of Disease Study 2010”. *The lancet*, vol. 380, no. 9859, pp. 2095–2128, 2012.
- [3] G. WHO. “Global tuberculosis report 2020”. *Glob. Tuberc. Rep*, 2020.
- [4] H. Sung, J. Ferlay, R. L. Siegel, M. Laversanne, I. Soerjomataram, A. Jemal and F. Bray. “Global cancer statistics 2020: GLOBOCAN estimates of incidence and mortality worldwide for 36 cancers in 185 countries”. *CA: a cancer journal for clinicians*, vol. 71, no. 3, pp. 209–249, 2021.
- [5] M. Molina-Molina, M. Aburto, O. Acosta, J. Ancochea, J. A. Rodríguez-Portal, J. Sauleda, C. Lines and A. Xaubet. “Importance of early diagnosis and treatment in idiopathic pulmonary fibrosis”. *Expert Review of Respiratory Medicine*, vol. 12, no. 7, pp. 537–539, 2018.
- [6] Q. Hu, L. F. d. F. Souza, G. B. Holanda, S. S. Alves, F. H. d. S. Silva, T. Han and P. P. Rebouças Filho. “An effective approach for CT lung segmentation using mask region-based convolutional neural networks”. *Artificial intelligence in medicine*, vol. 103, pp. 101792, 2020.
- [7] A. H. Sodhro, S. Pirbhulal and V. H. C. De Albuquerque. “Artificial intelligence-driven mechanism for edge computing-based industrial applications”. *IEEE Transactions on Industrial Informatics*, vol. 15, no. 7, pp. 4235–4243, 2019.
- [8] A. Mansoor, U. Bagci, B. Foster, Z. Xu, G. Z. Papadakis, L. R. Folio, J. K. Udupa and D. J. Mollura. “Segmentation and image analysis of abnormal lungs at CT: current approaches, challenges, and future trends”. *Radiographics*, vol. 35, no. 4, pp. 1056–1076, 2015.
- [9] P. P. Rebouças Filho, P. C. Cortez and M. A. Holanda. “Active contour modes crisp: new technique for segmentation of the lungs in ct images”. *Revista Brasileira de Engenharia Biomédica*, vol. 27, no. 4, pp. 259–272, 2011.
- [10] G. E. Batista, R. C. Prati and M. C. Monard. “A study of the behavior of several methods for balancing machine learning training data”. *ACM SIGKDD explorations newsletter*, vol. 6, no. 1, pp. 20–29, 2004.
- [11] R. C. Gonzalez and R. E. Woods. *Processamento de imagens digitais*. Editora Blucher, 2000.
- [12] Y. Xu, L. F. Souza, I. C. Silva, A. G. Marques, F. H. Silva, V. X. Nunes, T. Han, C. Jia, V. H. C. de Albuquerque and P. P. Rebouças Filho. “A soft computing automatic based in deep learning with use of fine-tuning for pulmonary segmentation in computed tomography images”. *Applied Soft Computing*, vol. 112, pp. 107810, 2021.
- [13] B. N. Li, J. Qin, R. Wang, M. Wang and X. Li. “Selective level set segmentation using fuzzy region competition”. *IEEE access*, vol. 4, pp. 4777–4788, 2016.
- [14] P. P. Rebouças Filho, A. C. da Silva Barros, J. S. Almeida, J. Rodrigues and V. H. C. de Albuquerque. “A new effective and powerful medical image segmentation algorithm based on optimum path snakes”. *Applied Soft Computing*, vol. 76, pp. 649–670, 2019.
- [15] N. Gupta, D. Gupta, A. Khanna, P. P. Rebouças Filho and V. H. C. de Albuquerque. “Evolutionary algorithms for automatic lung disease detection”. *Measurement*, vol. 140, pp. 590–608, 2019.
- [16] B. A. Skourt, A. El Hassani and A. Majda. “Lung CT image segmentation using deep neural networks”. *Procedia Computer Science*, vol. 127, pp. 109–113, 2018.
- [17] S. G. Armato III, G. McLennan, L. Bidaut, M. F. McNitt-Gray, C. R. Meyer, A. P. Reeves, B. Zhao, D. R. Aberle, C. I. Henschke, E. A. Hoffman *et al.*. “The lung image database consortium (LIDC) and image database resource initiative (IDRI): a completed reference database of lung nodules on CT scans”. *Medical physics*, vol. 38, no. 2, pp. 915–931, 2011.
- [18] T. Han, V. X. Nunes, L. F. D. F. Souza, A. G. Marques, I. C. L. Silva, M. A. A. F. Junior, J. Sun and P. P. Rebouças Filho. “Internet of medical things—based on deep learning techniques for segmentation of lung and stroke regions in CT scans”. *IEEE Access*, vol. 8, pp. 71117–71135, 2020.
- [19] E. S. Rebouças, R. M. Sarmiento and P. P. Rebouças Filho. “3D adaptive balloon active contour: method of segmentation of structures in three dimensions”. *IEEE Latin America Transactions*, vol. 13, no. 1, pp. 195–203, 2015.
- [20] G. L. B. Ramalho, D. S. Ferreira, P. P. Rebouças Filho and F. N. S. de Medeiros. “Rotation-invariant feature extraction using a structural co-occurrence matrix”. *Measurement*, vol. 94, pp. 406–415, 2016.

- [21] P. P. Rebouças Filho, P. C. Cortez, A. C. da Silva Barros and V. H. C. De Albuquerque. “Novel adaptive balloon active contour method based on internal force for image segmentation—a systematic evaluation on synthetic and real images”. *Expert Systems with Applications*, vol. 41, no. 17, pp. 7707–7721, 2014.
- [22] P. P. Rebouças Filho, P. C. Cortez, A. C. da Silva Barros, V. H. C. Albuquerque and J. M. R. Tavares. “Novel and powerful 3D adaptive crisp active contour method applied in the segmentation of CT lung images”. *Medical image analysis*, vol. 35, pp. 503–516, 2017.
- [23] Y. Wu, A. Kirillov, F. Massa, W.-Y. Lo and R. Girshick. “Detectron2”. <https://github.com/facebookresearch/detectron2>, 2019.
- [24] K. He, G. Gkioxari, P. Dollár and R. Girshick. “Mask r-cnn”. In *Proceedings of the IEEE international conference on computer vision*, pp. 2961–2969, 2017.
- [25] R. Girshick, I. Radosavovic, G. Gkioxari, P. Dollár and K. He. “Detectron”. <https://github.com/facebookresearch/detectron>, 2018.
- [26] D. Liu, Y. Zhao, A. K. Khambampati, A. Seppänen and J. Du. “A parametric level set method for imaging multiphase conductivity using electrical impedance tomography”. *IEEE Transactions on Computational Imaging*, vol. 4, no. 4, pp. 552–561, 2018.
- [27] E. Parzen. “On estimation of a probability density function and mode”. *The annals of mathematical statistics*, vol. 33, no. 3, pp. 1065–1076, 1962.
- [28] D.-Y. Yeung and C. Chow. “Parzen-window network intrusion detectors”. In *Object recognition supported by user interaction for service robots*, volume 4, pp. 385–388. IEEE, 2002.
- [29] A. A. Taha and A. Hanbury. “Metrics for evaluating 3D medical image segmentation: analysis, selection, and tool”. *BMC medical imaging*, vol. 15, no. 1, pp. 1–28, 2015.
- [30] P. Aljabar, R. A. Heckemann, A. Hammers, J. V. Hajnal and D. Rueckert. “Multi-atlas based segmentation of brain images: atlas selection and its effect on accuracy”. *Neuroimage*, vol. 46, no. 3, pp. 726–738, 2009.
- [31] A. K. Feeny, M. Tadarati, D. E. Freund, N. M. Bressler and P. Burlina. “Automated segmentation of geographic atrophy of the retinal epithelium via random forests in AREDS color fundus images”. *Computers in biology and medicine*, vol. 65, pp. 124–136, 2015.
- [32] H. Bhaduria and M. Dewal. “Intracranial hemorrhage detection using spatial fuzzy c-mean and region-based active contour on brain CT imaging”. *Signal, Image and Video Processing*, vol. 8, no. 2, pp. 357–364, 2014.
- [33] F. Milletari, N. Navab and S.-A. Ahmadi. “V-net: Fully convolutional neural networks for volumetric medical image segmentation”. In *2016 fourth international conference on 3D vision (3DV)*, pp. 565–571. IEEE, 2016.